

# **Neutron Capture Cross Sections of Cadmium Isotopes**

By  
Allison Gicking

A thesis submitted to  
Oregon State University

In partial fulfillment  
of the requirements for  
the degree of

Bachelor of Science

Presented June 8, 2011  
Commencement June 17, 2012

### **Abstract**

The neutron capture cross sections of  $^{106}\text{Cd}$ ,  $^{108}\text{Cd}$ ,  $^{110}\text{Cd}$ ,  $^{112}\text{Cd}$ ,  $^{114}\text{Cd}$  and  $^{116}\text{Cd}$  were determined in the present project. Four different OSU TRIGA reactor facilities were used to produce redundancy in the results and to measure the thermal cross section and resonance integral separately. When the present values were compared with previously measured values, the differences were mostly due to the kind of detector used or whether or not the samples were natural cadmium. Some of the isotopes did not have any previously measured values, and in that case, new information about the cross sections of these six cadmium isotopes has been provided.

## Table of Contents

I.	Introduction.....	1
II.	Theory.....	3
	1. Neutron Capture.....	3
	2. Resonance Integral vs. Effective Thermal Cross Section.....	5
	3. Derivation of the Activity Equations.....	8
III.	Methods.....	12
	1. Irradiation of the Samples.....	12
	2. Sample Preparation and Parameters.....	16
	3. Efficiency Calibration of Detectors.....	18
	4. Data Analysis.....	19
	5. Absorption by $^{113}\text{Cd}$ .....	20
IV.	Results.....	22
	1. Experimental Values.....	22
	2. Previous Values.....	24
	3. Comparison with Previous Values and Analysis.....	26
V.	Conclusions.....	32
VI.	References.....	34
VII.	Appendix.....	36
	1. Germanium Single Crystal Diode Detector.....	36
	2. Detector Efficiency Curves.....	38
	3. Neutron Fluxes.....	40
	4. Error Analysis.....	41
VIII.	Acknowledgments.....	43

## Chapter I: Introduction

Neutron activation analysis is a technique often used to determine the chemical composition of a substance. The process involves bombarding a material with neutrons and subsequently measuring the energy spectra of the gamma rays emitted. This type of analysis is used for determining the chemical composition of fragile pieces of art as well as historical objects. It is accomplished by having information about the likelihood that a nucleus will absorb a neutron and become radioactive. In other words, the neutron capture cross sections of the elements in the material need to be known. Neutron capture analysis is also imperative for the proper use of cadmium as a control rod in nuclear reactors. Therefore, accurately measuring the neutron capture cross sections of cadmium isotopes is an important contribution to the scientific community.

The neutron capture cross section of an atomic nucleus is not an actual cross-sectional area, but rather a measure of the probability of that nucleus absorbing a neutron and becoming radioactive. Therefore, it can be referred to as an “effective” cross section and it can be characterized by two different parameters: the resonance integral,  $I$ , and the thermal cross section,  $\sigma$ . The resonance integral is the sum of all the individual nuclear resonances over a range of high energies and the thermal cross section is the tail section of these resonances that can be simplified in a way that will be explained later. Both of the parameters are determined using the activation analysis method.

The activation analysis method involves measuring the emitted gamma ray peak areas, along with neutron fluxes, and calculating  $I$  and  $\sigma$  using an activity equation derived in Section II. Other parameters such as half-lives, branching ratios, activity levels, abundances and irradiation time also must be known. The cross-sections of the

isotopes of cadmium ( $^{106}\text{Cd}$ ,  $^{108}\text{Cd}$ ,  $^{110}\text{Cd}$ ,  $^{112}\text{Cd}$ ,  $^{114}\text{Cd}$  and  $^{116}\text{Cd}$ ) were determined in this way. The neutron source was the Oregon State University TRIGA reactor (OSTR) located at the OSU Radiation Center. TRIGA stands for *Training, Research, Isotopes, General Atomics* and is a type of reactor designed and manufactured by General Atomics. There were four different facilities used for the irradiations of the samples, each with different neutron flux characteristics. A program called Maestro was used to determine the peak areas and average activity levels.

Previous data that have been collected on the neutron capture cross-section of cadmium isotopes are compiled on the Brookhaven National Laboratory website [1]. There are several isotopes for which  $I$  and  $\sigma$  had never been measured and, in other cases, the values that did exist were not in good agreement with one another. Therefore, the motivation behind the measurements was to determine the cross sections and resonance integrals of cadmium isotopes as precisely as possible. This information can then be applied in areas such as neutron activation analysis and nuclear reactor control rods, as mentioned before.

When the procedure was carried out and the data analyzed, the initial numbers yielded two interesting anomalies. Firstly, all the samples gave different resonance integral results for two different irradiation facilities, indicating some inherent difference in the energy dependence of their respective neutron fluxes. And second, the thermal cross section values determined for  $^{114}\text{Cd}$  from the thermal column irradiation were consistently half as large as the values from the other three facilities. Otherwise, values within a reasonable amount of uncertainty were obtained successfully, and could be used in other experiments.

## Chapter II: Theory

### 2.1 Neutron Capture

To better understand the meaning of neutron capture cross sections it is important to know the nature of the neutron capture process itself. Neutron activation analysis requires bombarding a nucleus with a neutron to form a compound nucleus [2]. This compound nucleus is in a high-energy, or unstable, state. The nucleus would prefer to be in a stable state so it releases the extra energy in the form of electromagnetic radiation. This process is shown schematically in Fig. 2.1.

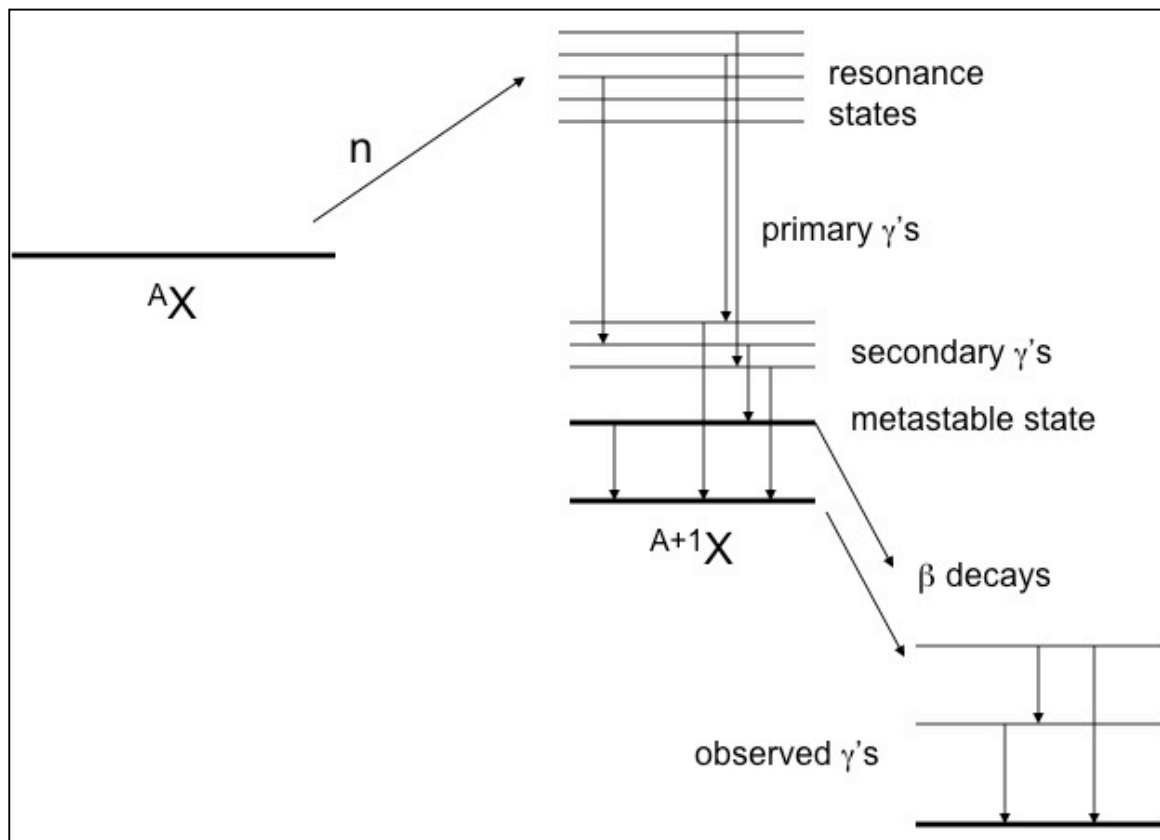


Figure 2.1: Decay scheme for the neutron capture process,  $^A X + n \rightarrow ^{A+1} X$ .

The decay process begins with primary gamma ray emission while the sample is still inside the reactor. These gamma rays have high energies ( $\sim 5$  MeV) and are emitted through transitions between energy levels with very short half-lives ( $< 10^{-15}$  seconds). However, at this point the nucleus is still unstable and emits secondary gamma rays to transition to even lower energy levels before it leaves the reactor.

Now the nucleus is either in a metastable state, which is an excited energy level close to the ground state, or a ground state. Metastable states generally have long half-lives due to their large nuclear spins. Photons emitted during transitions to different energy states want to carry as little angular momentum as possible (one or two units) so photons carrying three or four units of angular momentum are few and far between. Therefore, a transition between a state with a nuclear spin of  $1\frac{1}{2}$  and a state with a nuclear spin of  $\frac{1}{2}$  is going to occur much less often than a transition between  $3\frac{1}{2}$  and  $\frac{1}{2}$ . The metastable states usually emit gamma rays through photon transitions to the ground state.

In the case of the radioactive ground state, the nucleus transforms to a different element through either positive or negative beta decay ( $\beta$ ). Lighter Cd nuclei tend to  $\beta^+$  decay, which is the process by which an extra proton is converted into a neutron, and heavier Cd nuclei  $\beta^-$  decay, which is the process by which an extra neutron is converted into a proton. Light nuclei have a neutron deficiency and need the extra neutron, while heavy nuclei are already neutron rich. After  $\beta^-$  decay or  $\beta^+$  decay occurs, the excited state then decays to the ground state and the emitted gammas are measured. The result of this process is sometimes the formation of a new element, which in the case of cadmium

is either indium or silver. In other cases, such as  $^{115}\text{Cd}$  in the present work, the metastable state can also  $\beta$  decay.

However, before any of these processes can happen, the nucleus has to first absorb an incoming neutron. The chance of neutron capture is different for each target nucleus, depending on factors such as mass and spin. Therefore, the neutron capture cross section of an isotope can be defined as the probability of a reaction per incident neutron per target nucleus. It is an effective area of potential neutron absorption rather than an actual physical characteristic. This probability can be found indirectly by analyzing the gamma ray emission spectra with the procedure described in Chapter III.

## **2.2 Resonance Integral vs. Effective Thermal Cross Section**

These cross sections are described by two separate characteristics: the thermal neutron cross section and the resonance integral. For the purpose of measuring the cross sections of cadmium isotopes both thermal and epithermal neutrons were captured. Thermal neutrons have a characteristic energy of about 0.025 eV, but they technically range from 0 to  $\sim 1$  eV. Epithermal neutrons have energies ranging from 1 eV to 10 keV. There are also very fast neutrons with an energy range of  $>10$  keV, but the interactions they participate in are not very probable and were not taken into account in this procedure.

The thermal cross section is the effective cross section value associated with the absorption of neutrons with energies in the thermal range. For neutrons within this energy range, the cross section of the target depends on  $1/v$  where  $v$  is the speed of the incoming



neutron [3]. This simple relationship can be determined from the Breit-Wigner formula for the reaction  $a + X \rightarrow b + Y$ :

$$\sigma = \frac{\pi}{k^2} g \frac{\Gamma_n \Gamma}{(E_R - E)^2 + \frac{\Gamma^2}{4}} \quad (2.1)$$

where  $k$  is the momentum,  $\Gamma$  is an energy width that represents the likelihood of gamma decay,  $\Gamma_n$  is an energy width that represents the likelihood of neutron capture,  $E_R$  is the resonance energy, and  $E$  is the kinetic energy of the incoming neutron. Only the  $\Gamma_n$  is dependent on the velocity of the incoming neutron, due to the high probability of gamma decay. Also, the neutron's kinetic energy,  $E$ , can be considered negligible compared to the resonance energy,  $E_R$ . The velocity dependence of the  $\Gamma_n$  cancels with the velocity dependence of  $k$  to give a final result of

$$\sigma \propto \frac{1}{v} \quad (2.2)$$

This is a very important result because it greatly simplifies the factors affecting the thermal cross section, which makes the value much easier to measure. Since the velocity dependence is simply an inverse relationship, the thermal cross section can be determined without summing resonances.

Incoming epithermal neutrons cause the target nucleus to enter resonance states that will eventually decay to the ground state. The sum of all these individual resonance peaks is called a resonance integral,  $I$ . The tail of these resonances, caused by lower energy neutrons, contribute to the thermal cross section,  $\sigma$ . Fig. 2.2 is a sample plot of the neutron capture cross section as a function of neutron energy for the  $^{110}\text{Cd} \rightarrow ^{111\text{m}}\text{Cd}$  transition. The plot can easily be divided into three sections, which correspond to the thermal, epithermal and fast energy ranges.

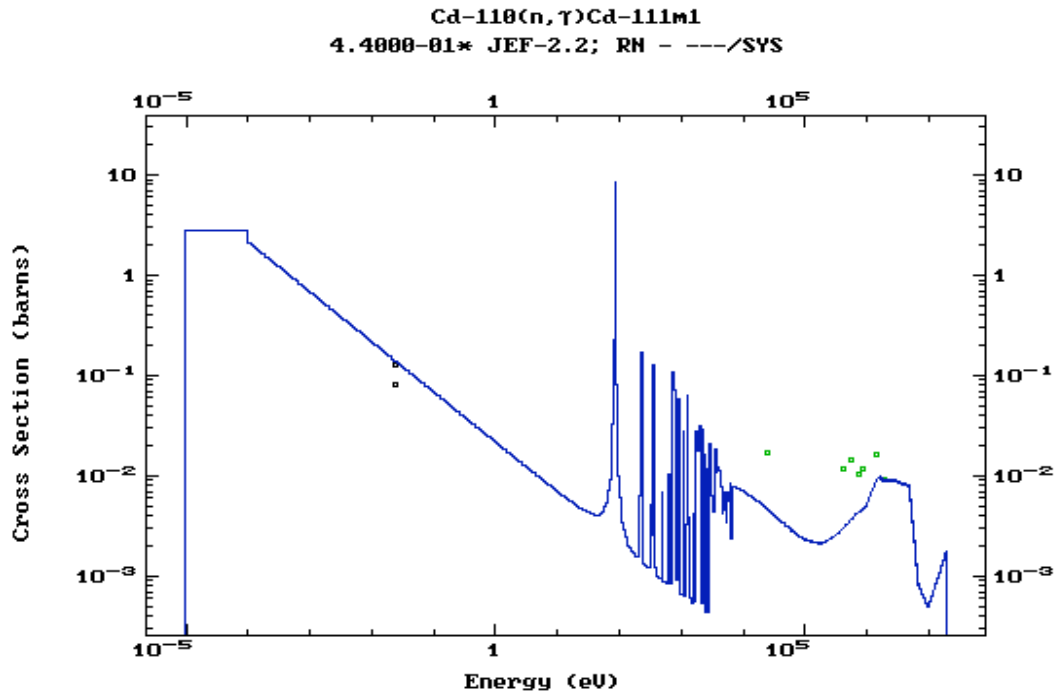


Figure 2.2: Cross section as a function of energy for  $^{110}\text{Cd}$ . There are three distinct regions representing thermal, epithermal and very fast neutrons (left to right).

The thermal region integral can be simplified to a  $v^{-1}$  dependence, due to the Breit-Wigner formula, and it becomes the thermal cross section,  $\sigma$ , value. The resonances in the epithermal region are more complicated and can not be determined individually, therefore their sum is the resonance integral value,  $I$ . Very fast neutrons can be ignored because both the cross section and the flux decrease in this energy range.

Fig. 2.2 shows how the neutron capture cross section of the  $^{110}\text{Cd}$  nucleus is dependent on the energy, or velocity, of the incoming neutron. However, the same plot for  $^{113}\text{Cd}$ , shown in Figure 2.3, demonstrates why separated isotopes needed to be used.

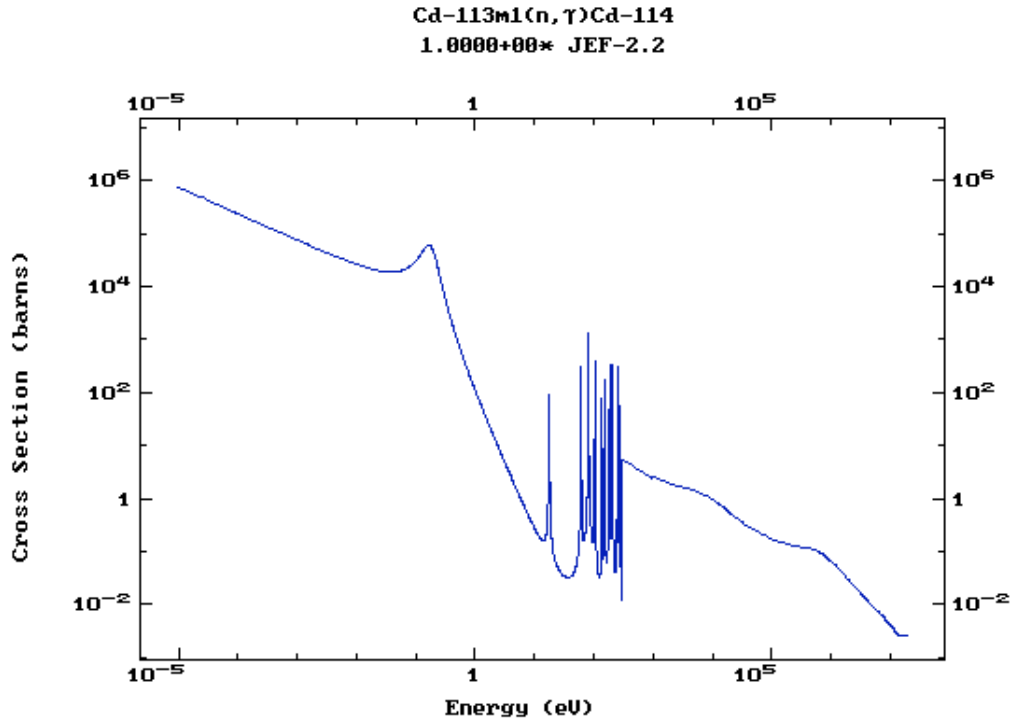


Figure 2.3: Energy dependence of the cross section of  $^{113}\text{Cd}$

The cross sections for the thermal neutron region no longer have a  $v^{-1}$  dependence and they are significantly larger than cross sections of other cadmium isotopes. This problem of high absorption probability in the lower energy ranges can be mitigated by using separated isotopes of cadmium. In natural cadmium, there is 12% of  $^{113}\text{Cd}$ , which can greatly skew the cross section value if it is not taken into account. If there is no  $^{113}\text{Cd}$  to absorb all the thermal neutrons, a more accurate value for the cross sections can be determined.

### 2.3 Derivation of the Activity Equations

A capture cross section cannot be measured directly, it can only be calculated using other measured values. In this case, the measured values were the activities of the

samples and the neutron fluxes of the irradiation facilities. The activity can be found starting with the equation for reaction rate:

$$R = N_0 \sigma \varphi_{th} \quad (2.3)$$

For the purpose of this experiment,  $R$  can be considered a constant with respect to time.

$N_0$  is the number of atoms present in the sample and it varies a negligible amount because the number of atoms originally present greatly outnumbers the atoms being created.

Lastly, the  $\sigma \varphi_{th}$  term is a representation of the thermal neutrons being absorbed, where  $\sigma$  is the thermal cross section and  $\varphi_{th}$  is the thermal flux (see Appendix 6.2). Both of these values remain constant for a particular isotope throughout the neutron capture process.

An adjustment of Eq. 2.3 needs to be made in order to account for the incoming epithermal neutrons mentioned in Section 2.2.

$$R = N_0 (\sigma \varphi_{th} + I \varphi_{epi}) \quad (2.4)$$

where  $\varphi_{epi}$  is the epithermal neutron flux.

It is also important to account for the overall change in the number of atoms due to radioisotopes being simultaneously produced and destroyed. The change in the number of atoms,  $N$ , with respect to time can be represented as

$$dN = Rdt - \lambda Ndt \quad (2.5)$$

where  $\lambda$  is the exponential decay constant determined by the reciprocal of the average lifetime of the element. Therefore,  $Rdt$  is the number of atoms being created due to neutron capture and  $\lambda Ndt$  is the number of atoms being eliminated due to radioactive decay. Subtracting the number of atoms being eliminated from the number of atoms being created gives the change in the total number of atoms at any given time during a reaction.

Eq. 2.5 can then be put in the form,

$$\frac{dN}{dt} = R - \lambda N$$

Solving this differential equation for  $N(t)$  gives:

$$N(t) = \frac{R}{\lambda}(1 - e^{-\lambda t})$$

In order to solve for the cross section,  $N(t)$  needs to be related to the activity. The activity is defined as the decays per second in the sample and can be represented symbolically as

$$A = \lambda N(t) = R(1 - e^{-\lambda t})$$

And finally, the activity and the cross section can be related to one another

$$A = N_0(\sigma\varphi_{th} + I\varphi_{epi})(1 - e^{-\lambda t}) \quad (2.6)$$

Eq. 2.6 is the fundamental relationship used to solve for the thermal cross sections and resonance integrals.

Since  $\sigma$  and  $I$  are being solved for, and all the other parameters are known, the activity,  $A$ , needs to be determined for each isotope. This can be done using

$$A = \frac{N}{\epsilon b T} \quad (2.7)$$

where  $b$  is the branching ratio, or the relative intensity of each gamma ray,  $\epsilon$  is the detector efficiency (see Chapter III) and  $T$  is the counting time. However, this is the activity at time  $t_d$  after the sample was removed from the reactor and not the end of bombardment (EOB) activity. The EOB activity can be found by dividing  $A$  by the decay factor to get

$$A = \frac{N}{e^{-\lambda_d t_d} \epsilon b T} \quad (2.8)$$

Setting Eq. 2.8 equal to the result of Eq. 2.6 and solving for either  $\sigma$  or  $I$  is the process followed for all the cross section values. It will be discussed in more detail in Chapter III.

## Chapter III: Methods

### 3.1 Irradiation of the Samples

Finding the neutron capture cross-section of an isotope requires irradiating a source and counting the emitted gamma rays. All irradiations took place at the Oregon State TRIGA Reactor (OSTR).

There were four different facilities at OSTR used for irradiation: the cadmium lined in-core irradiation tube (CLICIT), the pneumatic transfer tube (Rabbit), the thermal column (TC), and the g-ring in-core irradiation tube (GRICIT). The CLICIT facility sees only epithermal neutrons due to its cadmium lining and was used for measurements needed to find the resonance integral. The Rabbit facility is located close to the core itself and was used primarily for short irradiations of isotopes with short half-lives (1-10 minutes). Wrapping some samples in cadmium before irradiating them in the Rabbit allowed only epithermal neutron flux and the resonance integral could be directly measured. The TC has no cadmium lining and therefore, the samples irradiated in this facility were subject to both thermal and epithermal neutrons, but the epithermal flux is so small it can be considered negligible. This facility was used for measurements needed to determine the effective thermal cross section. Finally, the GRICIT has both epithermal and thermal neutron flux and was used to measure the thermal cross sections of isotopes with relatively long half-lives. Both the resonance integral and thermal cross section values were cross-checked for each isotope due to the redundancy in irradiation.

Once the samples were removed from the irradiation facility they were placed in front of a detector at a distance from 10-20 cm. The time between removing the irradiated samples from the facility and placing them in front the detector ranged from minutes to

hours. The spectra data from the detectors were analyzed using a program called Maestro. Maestro displayed the gamma ray spectrum for each isotope, as well as recorded the number of counts for each gamma ray by measuring the area under each peak. These data were then consolidated and used to calculate the cross sections and resonance integrals themselves. Fig. 3.1-5 are sample gamma ray spectra created by Maestro for each isotope. These spectra were analyzed to find the relevant cross section values using the procedure outlined in Section 3.4 below.

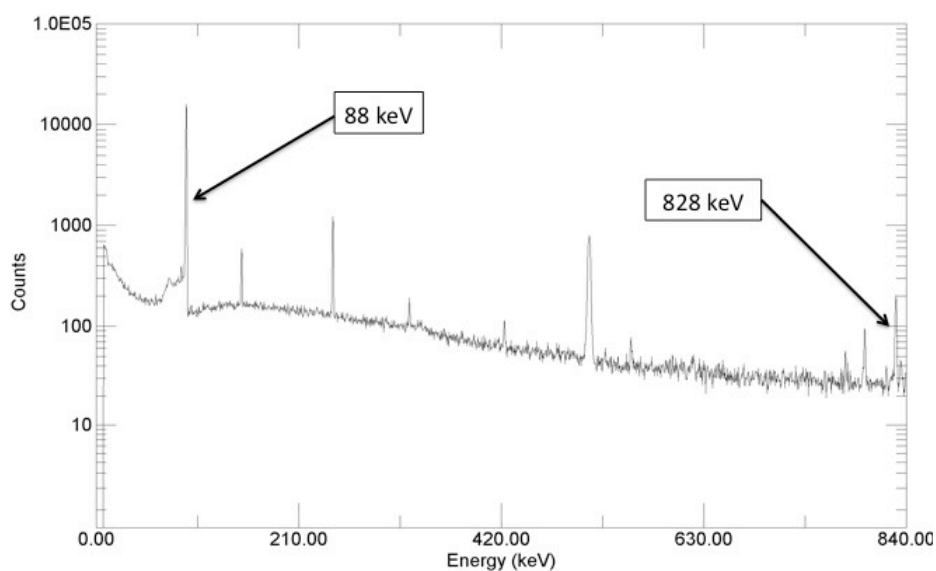


*Figure 3.1: Gamma ray spectrum for  $^{107}\text{Cd}$  and  $^{109}\text{Cd}$  (Sample A) created by the program Maestro. The relevant gamma rays are labeled on the figure.*



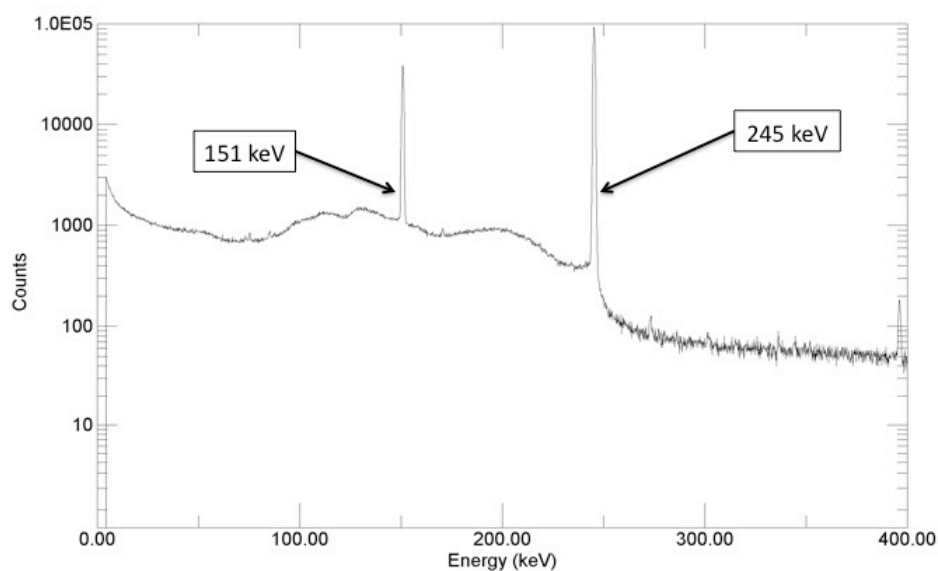


Figure 3.2 Gamma ray spectrum for  $^{111}\text{Cd}$  (Sample B) created by Maestro. The relevant gamma ray peaks are 150 keV and 245 keV as indicated on the figure.

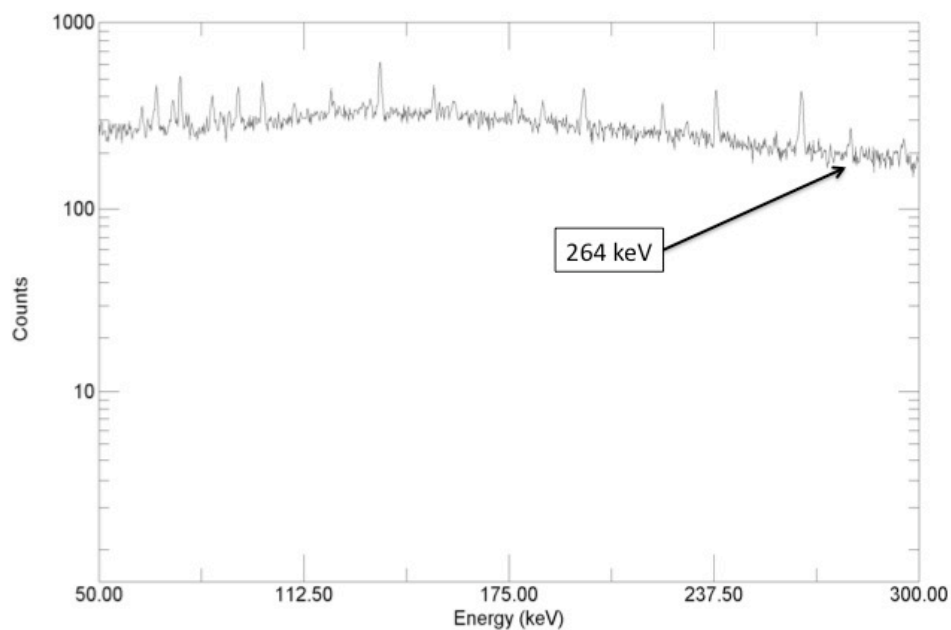


Figure 3.3: Gamma ray spectrum for  $^{113}\text{Cd}$  (Sample C) created by Maestro. The relevant gamma ray is labeled.

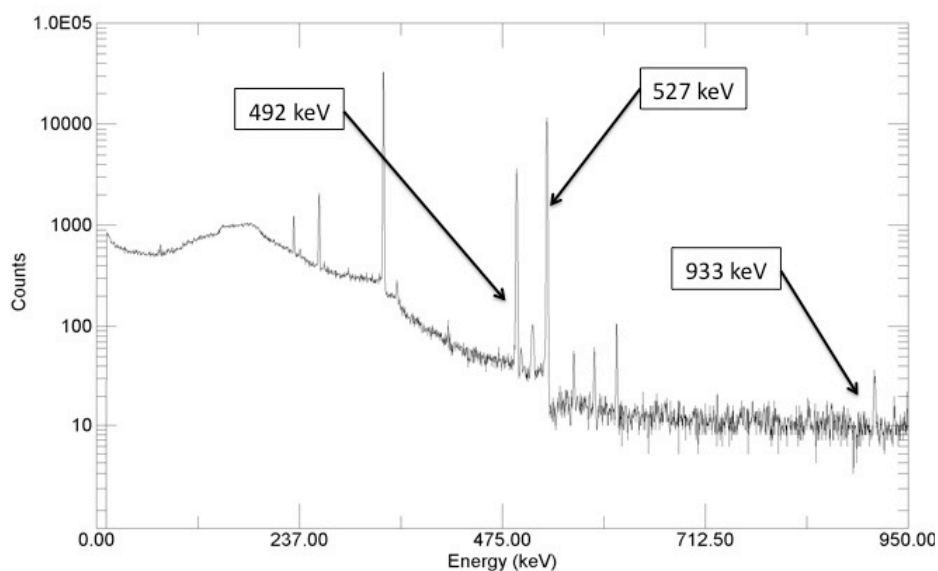


Figure 3.4: Gamma ray spectrum for  $^{115}\text{Cd}$  (Sample D) created by Maestro. The relevant gamma rays are labeled.

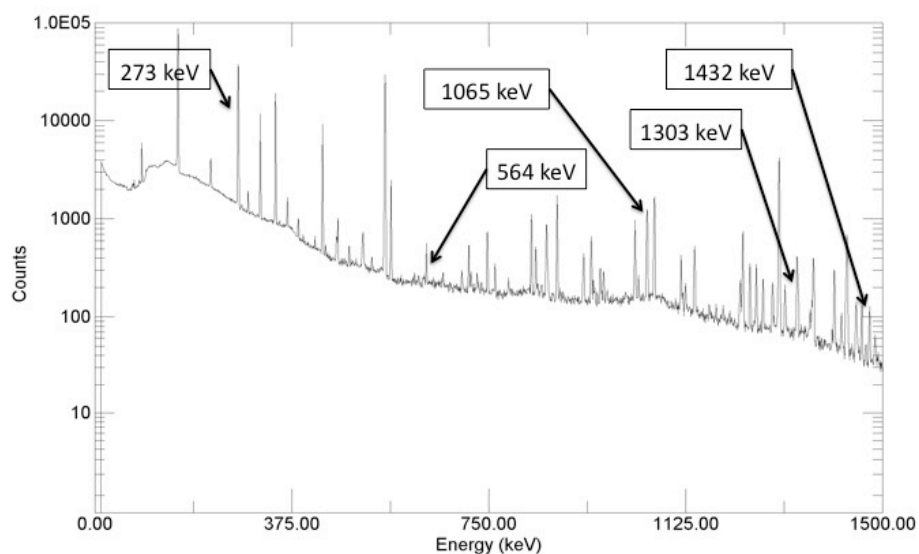


Figure 3.5: Sample gamma ray spectrum for  $^{117}\text{Cd}$  (Sample E) created by Maestro. The relevant gamma rays are labeled.

### 3.2 Sample Preparation and Parameters

Separated isotopes of cadmium were used to eliminate the effects of  $^{113}\text{Cd}$ 's large capture cross section. The  $^{108}\text{Cd}$  sample contained about 90% of  $^{108}\text{Cd}$  and about 6% of  $^{106}\text{Cd}$ , which was enough to perform the experiment. Therefore, Sample A contained two isotopes. Samples B and E were  $^{110}\text{Cd}$  and  $^{116}\text{Cd}$ , respectively, and were also cadmium metal pieces. Lastly, samples C and D correlating to  $^{112}\text{Cd}$  and  $^{114}\text{Cd}$  were cadmium oxide powders. The abundances for each sample, A through E, are compiled in Table 3.1. Each sample was carefully weighed out and placed in an aluminum packet before being placed in each irradiation facility. The masses ranged from 4-40 mg depending on the form and quantity available. Table 3.2 contains the masses for each sample in each irradiation facility as well as the run times in the facilities themselves.

*Table 3.1: Abundance of cadmium isotopes in each cadmium sample.*

	106	108	110	111	112	113	114	116
A	6.15	90.7	3.1	<0.05	<0.05	<0.05	<0.05	<0.05
B	0.01	0.01	95.6	1.09	1.42	0.52	1.17	0.18
C	<0.01	<0.01	0.13	0.41	98.23	0.64	0.52	0.05
D	<0.01	<0.01	<0.01	0.01	0.03	0.6	98.6	0.3
E	<0.05	<0.05	<0.05	<0.05	<0.05	<0.05	1.23	98.77

The data analysis, described in Section 3.4, required the knowledge of the half-lives of each isotope and the branching ratios for each gamma ray. These values are compiled in Table 3.3. The sources and uncertainties of these values are discussed in detail in Appendix 6.4.

*Table 3.2: The irradiation times for each facility and the sample masses for each facility. There are blanks because not all samples were irradiated in all of the facilities due to the nature of their half-lives or cross sections.*

Facility	CLICIT	Rabbit 1	GRICIT	Rabbit 2 (Cd)	Rabbit 3	Rabbit 4 (Cd)	Thermal Column
Irradiation Time	1 h	10 min	1 h	5 min	10 min	5 min	2 h
Mass of Sample for each facility (milligrams)							
A	4.0		3.6		4.4	4.8	5.1
B	4.0	4.0	3.4	4.9		4.0	5.0
C	39.9		26.8				
D	13.5	7.7	13.7	8.5			29.3
E	4.1	3.1	4.2	7.25			5.2

*Table 3.3: The half-lives for each radioisotope and branching ratios for all the gammas used in the cross section analysis for cadmium isotopes.*

Capturing Isotope	Radioisotope	Half-life	Gamma Energy (keV)	Branching Ratio (%)
106	107	6.5 h	828	0.16
108	109	462.2 d	88	3.61
110	111	48 min	151	29.1
			245	94
112	113m	14 y	264	0.02
114	115g	2.23 d	492	8.03
			527	27.45
114	115m	44.6 d	933	2.0
116	117g	2.49 h	273	28
			1303	18.4
116	117m	3.36 h	564	14.7
			1065	23.1
			1432	13.4

### 3.3 Efficiency Calibration of Detectors

The neutron capture cross sections of six isotopes of cadmium were determined using three germanium single crystal diode gamma ray detectors (see Appendix 6.1). Each detector had an efficiency function that was calculated for a range of energies at several different distances from the source, as shown in Fig. 3.6.

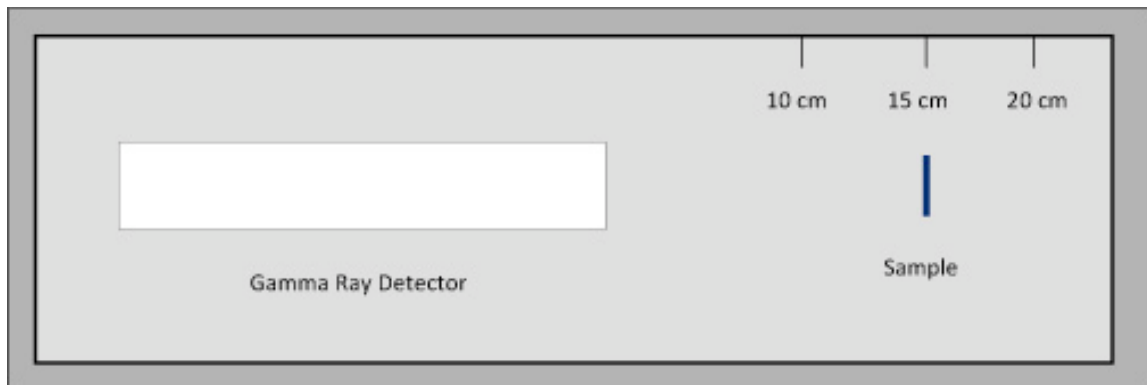


*Figure 3.6: Schematic diagram of the gamma ray detector and source set-up. The dark edges represent the lead bricks used to prevent the detector from picking up gamma rays from other sources.*

Efficiency, in this case, means the probability that a gamma ray is going to enter the detector and be counted towards the total peak area. To accomplish calibrating these efficiencies, two isotopes with known gamma ray energy levels, branching ratios and activities were used as sources;  $^{152}\text{Eu}$  and  $^{133}\text{Ba}$ . They were placed 10, 15 and 20 cm from a detector and counted for approximately 1-2 days. The count number and run time were recorded and used to solve the following equation for efficiency:

$$\varepsilon = \frac{N}{AbT} \quad (3.1)$$

In the above equation,  $N$  is the count number,  $T$  is the run time,  $A$  is the current activity level and  $b$  is the branching ratio. The activity level could be calculated using the

exponential equation:  $A(t) = A_0 e^{-\lambda t}$  and the branching ratios were found in the Nuclear Data Sheets (NDS) [4].

Once the efficiency functions for each detector were determined, a plot of the efficiency vs. energy was made. The barium isotopes were used for the lower energy (70-400 keV) calibrations and the europium was used for the higher energy (400-1400 keV) calibrations. The calibrated values were combined on a log-log plot, which gave a clearer, functional representation of the relationship between energy and efficiency. Using the high and low energy efficiency plots and their corresponding functions, the efficiency of a detector for any gamma ray energy could be determined precisely. This process is described in more detail in Appendix 6.2.

### 3.4 Data Analysis

Along with energy values, counts and uncertainties, Maestro recorded the date and time of the run, dead time, and live time for each sample while it was interacting with the detector. The actual cross sections and resonance integrals themselves were calculated using Microsoft Excel spreadsheets as analysis templates. These spreadsheets contained all the parameters used in the activity equations described in Chapter II.

First, the end of bombardment (EOB) activity of the sample was calculated by solving Eq. 2.6. Setting the result for EOB activity equal to the activity Eq. 2.8 gives an equation for which  $I$  and  $\sigma$  are the only unknowns. In order to isolate and solve for  $\sigma$  or  $I$ , the thermal or epithermal flux needed to be known. The procedure for calculating the fluxes is outlined in Appendix 6.3. For the rabbit samples with cadmium enclosed in a cadmium container and the CLICIT, the thermal flux could be set to zero and removed

from the equation. The Rabbit samples with no cadmium container and GRICIT samples experienced both types of fluxes, so the resonance integral value for the other samples needed to be used to obtain  $\sigma$ . In the case of the thermal column, the epithermal flux is negligible and therefore, has a very small effect on the thermal cross section value.

Lastly, a small correction needed to be made to the resonance integral value to correct for the contribution from the thermal neutrons. As mentioned in the theory section, the Breit-Wigner formula shows that the cross section of a thermal neutron has a dependency of  $1/v$ , where  $v$  is the neutron's incoming speed. However, there are some thermal neutrons that also exist in the epithermal neutron region, leading to an extra addition of neutrons used to calculate the resonance integral. This is equal to  $0.45\sigma$  [5] and the effective resonance integral can be calculated using

$$I_{eff} = I + 0.45\sigma \quad (3.3)$$

The corrected value for the resonance integral can then be used to determine the thermal cross section.

### 3.5 Absorption by $^{113}\text{Cd}$

Even though separated isotopes were used in the present experiment, there was still a non-negligible amount of  $^{113}\text{Cd}$  in samples B, C and D. Therefore, it was necessary to calculate the possible effect the presence of  $^{113}\text{Cd}$  would have on the cross section values. The calculation involves determining the attenuation of the intensity of the neutron beam by  $^{113}\text{Cd}$ , starting with Eq. 3.4.

$$I = I_0 e^{-n\alpha x} \quad (3.4)$$

where  $n$  is the atomic density,  $\sigma$  is the neutron capture cross section and  $x$  is the thickness of the sample. The atomic density can be estimated by determining the number of moles per unit volume, and multiplying by Avogadro's number. For the present experiment that attenuations for samples B, C and D were 22, 26 and 3 % respectively. This means that the attenuation was negligible for sample D and needed to be taken into account for samples B and C.



## Chapter IV: Results

### 4.1 Experimental Values

All the results obtained in this experiment are compiled in Tables 4.1 and 4.2 below. Both the resonance integral,  $I$ , and the thermal cross section,  $\sigma$ , values are given for each isotope.

*Table 4.1: A compilation of the experimental results for the resonance integrals of cadmium isotopes, for all the different irradiation facilities. Uncertainties are in parentheses.*

Resonance Integral (I, barns)					
	CLICIT	CLICIT 2	R2	R4	R10
<b>106→ 107 5/2+</b>	7.59(46)			6.6(5)	6.9(5)
<b>108→ 109 5/2+</b>	7.39(34)			5.0(2)	
<b>110→ 111m 11/2-</b>	0.788(36)	0.753(34)	0.58(3)	0.61(3)	
<b>112→ 113m 11/2-</b>	1.00(8)				
<b>114→ 115g 1/2+</b>	6.73(25)	6.38(24)	3.8(1)		3.7(1)
<b>114→ 115m 11/2-</b>	0.537(189)		0.39(14)		
<b>116→ 117g 1/2+</b>	1.35(5)	1.33(5)	1.07(4)		1.17(4)
<b>116→ 117m 11/2-</b>	0.423(15)	0.412(14)	0.30(1)		0.33(1)

*Table 4.2: A compilation of the experimental results for the thermal cross sections of cadmium isotopes, for all the different irradiation facilities. Uncertainties are in parentheses.*

<b>Thermal Cross Section (<math>\sigma</math>, barns)</b>							
	<b>TC</b>	<b>TC2</b>	<b>TC3</b>	<b>GRICIT</b>	<b>R1</b>	<b>R3</b>	<b>R9</b>
<b>106→ 107 5/2+</b>	0.817(70)			0.852(56)		0.871(56)	0.765(49)
<b>108→ 109 5/2+</b>	0.304(17)			0.314(18)		0.351(17)	
<b>110→ 111m 11/2-</b>	0.047(2)			0.057(3)	0.055(3)		0.0534(2)
<b>112→ 113m 11/2-</b>				0.037(3)			
<b>114→ 115g 1/2+</b>	0.272(10)	0.270(10)	0.276(10)	0.61(2)	0.531(20)		0.51(20)
<b>114→ 115m 11/2-</b>	0.027(9)			0.049(18)	0.041(15)		
<b>116→ 117g 1/2+</b>	0.0835(30)			0.091(3)	0.0895(31)		0.087(3)
<b>116→ 117m 11/2-</b>	0.0162(6)			0.0158(7)	0.0164(6)		0.0166(6)

Simply looking at Tables 4.1 and 4.2 reveals several obvious characteristics of the data. Firstly, the captures leading to higher spin values have much smaller cross sections and resonance integrals than the transitions with low spin values. This is due to the fact that most metastable states have high spin values, such as 11/2, and the resonance states have very low spin, such as 1/2. When radiation is emitted in a transition between energy states, it likes to carry the least amount of angular momentum as possible, about two units or less. In this case, this radiation is the gamma rays resulting in the transition from the resonance states to lower excited states. This means there aren't as many gamma rays that carry enough momentum to change the angular momentum of the nucleus by four units,

such as with  $110 \rightarrow 111m$  transition that has an angular momentum of  $11/2$ . Therefore, it makes sense that these neutron capture processes would be much less likely.

The second important observation to make is that the CLICIT resonance integrals do not agree with the resonance integrals determined from the Rabbit facility. Also, the results for  $^{114}\text{Cd}$  taken from the thermal column and GRICIT samples both have some anomalies when compared to the Rabbit data. It is difficult to surmise the source of these discrepancies when there is no information available about the energy dependence of the fluxes of the irradiation facilities.

## 4.2 Previous Values

All the previous values that have been measured or calculated in the past 100 years are compiled in Table 4.3. The top line in both sections corresponds to the accepted values compiled by Mughabghab [5]. Many of the values can be considered to hold less weight because they were measured during a time when high-resolution detectors were not available, which is anytime before the 1960's. Also, many values have large uncertainties and other problems that will be discussed in more detail later on in this section.

*Table 4.3: Compilation of previously measured and/or calculated values for the resonance integrals and thermal cross sections of cadmium isotopes. (Calculated values are denoted by an \* and Mughabghab's values are the first row of numbers for both sets.)*

Resonance Integrals							
107	109	111m	113	115g	115m	117g	117m
4.1*	10.7*	3.9(1)		12.5(10)*		1.5(2)*	
	16.7(46) <sup>a</sup>	3.92(10) <sup>c</sup>	0.043(10) <sup>l</sup>	3.16(159) <sup>e</sup>		0.42(25) <sup>e</sup>	
	12(2) <sup>b</sup>	2.0(1) <sup>d</sup>	0.760(193) <sup>m</sup>	14.1(7) <sup>c</sup>			
				3.4(2) <sup>d</sup>			
				23.3(2) <sup>j</sup>			
Thermal Cross Sections							
1*	0.72(13)	0.035(2)		0.294(16)	0.036(7)	0.050(8)	0.025(10)
	1.41(35) <sup>f</sup>	0.132(20) <sup>f</sup>	0.028(2) <sup>m</sup>	0.294(16) <sup>c</sup>		0.050(8) <sup>k</sup>	0.027(5) <sup>k</sup>
	2.7(9) <sup>a</sup>	0.082(8) <sup>i</sup>		0.300(15) <sup>j</sup>			
	1.1(1) <sup>g</sup>	0.035(2) <sup>c</sup>					
	24(10) <sup>h</sup>						
	0.20(3) <sup>b</sup>						

<sup>a</sup>Beda, A. [7]

<sup>b</sup>Anufriev, V. [6]

<sup>c</sup>Heft, R.E. [10]

<sup>d</sup>Van der Linden, R. [11]

<sup>e</sup>Sage, L. [15]

<sup>f</sup>Mangal, S. [9]

<sup>g</sup>Lewis, [18]

<sup>h</sup>Boyd, H. [8]

<sup>i</sup>Kramer, H.H. [12]

<sup>j</sup>Pearlstein, [19]

<sup>k</sup>Decat [17]

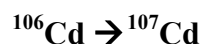
<sup>l</sup>Wahl [14]

<sup>m</sup>Nakamura, S. [13]

### 4.3 Comparison with Previous Values and Analysis

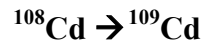
It is important to note that the values found for resonance integrals and thermal cross sections in this experiment are different from the values compiled in Table 4.3. The reason the data collected hold more weight than the previously measured data is due to several factors: advances in technology, the use of separated isotopes and redundancy. Before the 1960's, high-resolution detectors, such as the germanium single crystal diode detector used in these experiments, were not available. This made it hard to observe specific gamma ray peaks, especially if they had small intensities and branching ratios. Cadmium, especially, is a difficult element for which to measure neutron capture cross sections because of  $^{113}\text{Cd}$ . This specific isotope has an effective cross section that is so large it absorbs almost all incoming thermal neutrons, rendering any chance of measuring the thermal cross section to be difficult. Unless separated isotopes were used, this large absorption effect would greatly skew the results. Lastly, the samples in the present experiment were irradiated in many different facilities that used thermal neutron fluxes, epithermal neutron fluxes or both. Therefore, agreement between the cross section values for different facilities and irradiation times is a good indication that they are close to the correct value.

It is still necessary, however, to consider exactly why such discrepancies exist between presently and previously measured values for each isotope.



As evidenced by Table 4.3, the only known previous values of the resonance integral and thermal cross section of  $^{106}\text{Cd}$  are Mughabghab's calculated values of 4.1 b and 1 b, respectively. Both of these values are similar to the presently measured experimental

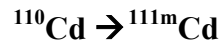
values of  $\sim 6.5$  b and  $\sim 0.8$  b. The cross section values obtained for  $^{106}\text{Cd}$  in the present experiment are the first measured values for this particular isotope.



It is unclear where the Mughabghab value comes from for the  $^{108}\text{Cd}$  cross section. The most recent experimental values were determined in 1984 by V.A. Anufriev [6] using enriched cadmium samples containing 5% of the highly absorbent  $^{113}\text{Cd}$  isotope. Anufriev used an internal conversion method for his values of  $0.20 \pm 0.03$  b for the thermal cross section and  $12 \pm 2$  b for the resonance integral. Internal conversion is a process by which an electron is emitted instead of a gamma ray or photon, so the results obtained through this method should not differ greatly from the present results. Data obtained in 1981 by A.K. Beda [7] also came from enriched cadmium samples containing about 5% of  $^{113}\text{Cd}$ . His values for the resonance integral and thermal cross section were  $16.7 \pm 4.6$  b and  $2.7 \pm 0.9$  b, respectively, which do not agree with the presently measured values of  $\sim 5$  b and  $\sim 0.3$  b. Beda did also use an activation method but he did not use high-resolution detectors, which would compromise his values. The uncertainty of up to 30% in Beda's  $\sigma$  value is indicative of this problem. He also used the activity ratio of  $^{115}\text{Cd}$  to  $^{109}\text{Cd}$  in one sample to find the cross section instead of measuring each cross section individually. Beda used a previously measured value of  $\sim 1.1$  b for the  $^{114}\text{Cd}$  cross section in his calculations to find the cross section of  $^{108}\text{Cd}$ , but the presently measured value is  $\sim 0.5$  b, thus, another reason for any discrepancy.

There are two other values for the thermal cross section of  $^{109}\text{Cd}$ , measured by Boyd [8] and Mangal [9] in the early sixties. Their respective values of  $1.41 \pm 0.35$  b and  $24 \pm 10$  b do not agree very well with the presently measured value of  $\sim 0.3$  b. Both of

these experiments relied on internal conversion, naturally occurring cadmium samples and low-resolution detectors. In fact, the values obtained for both the  $I$  and  $\sigma$  of  $^{108}\text{Cd}$  in the present experiment were the first values found using high-resolution detectors and separated isotopes.



The resonance integral and thermal cross section for  $^{110}\text{Cd}$  were both measured by Heft [10] in 1978. Mughabghab used these experimental values of  $0.035 \pm 0.002$  b for the thermal cross section and  $3.9 \pm 0.1$  b for the resonance integral in his compilation. The thermal cross section value is in good agreement with the presently measured value of  $\sim 0.05$  b but the resonance integral value is not in agreement with the present value of  $\sim 0.6$  b. Heft doesn't go into detail about the procedure he used in his paper but he does mention that he used natural cadmium samples. Whether or not Heft accounted for the high absorption of  $^{113}\text{Cd}$  in these experiments is unknown. Van der Linden also determined the resonance integral using natural cadmium and high-resolution detectors [11]. His value of  $2.0 \pm 0.1$  b was derived from a ratio of cross sections instead of individual measurements, similar to what Beda did to determine the cross section of  $^{108}\text{Cd}$ . He also used a  $\sigma$  value of 0.1 for his calculations, instead of 0.5 b, as indicated by the present experiments. Had he used the new value of  $\sigma$ , his result for the  $I$  would be very similar to the new result.

The last two values that exist for the thermal cross section of  $^{110}\text{Cd}$  were measured by Mangal [9] and Kramer [12] in the early sixties. Their values of  $0.132 \pm 0.020$  b and  $0.082 \pm 0.008$  b are not in agreement with the presently measured values. The fact that the previous measurements were taken in the sixties implies the use of low-resolution

detectors and therefore, less accurate results. Also, Kramer used an enriched sample of the isotope but failed to take the possibility of inelastic scattering into account. Inelastic scattering was negligible in the present experiment due to the fact that there was a negligible amount of  $^{111}\text{Cd}$  in the  $^{110}\text{Cd}$  sample.



There is one previously measured value for the I of  $^{112}\text{Cd}$ , which was obtained by Nakamura [13] in 2009. Nakamura's value of  $0.760 \pm 0.193$  b differs from the presently measured value of 1.0 b but not by more than a standard deviation. Since the procedure Nakamura used in his experiments was similar to the procedure used in the present experiment, the agreement between the two sets of values is a good indication of accuracy.

There are two previously measured values for the thermal cross section of this interaction. Wahl [14] obtained the earliest previously measured value of  $0.043 \pm 0.010$  b for  $\sigma$  in 1959, when there were no high-resolution detectors available. Therefore, his result can be considered to hold less weight than the presently measured results. Nakamura's value of  $0.0281 \pm 0.0021$  b also differs from the presently measured value of 0.037 b.



For his compilation, Mughabghab used Heft's [10] value of  $0.294 \pm 0.016$  b for the  $\sigma$ , and a calculated value of  $12.6 \pm 1.0$  b for the I. The calculated value is actually the sum of the cross sections for the ground and isomeric states, rather than just the ground state. Van der Linden also measured the resonance integral and his value of  $3.4 \pm 0.2$  b is in good agreement with the current value of 3.72 b. Sage's [15] value of  $3.16 \pm 1.59$  b is



also within 20% of the current value and it has a 50% uncertainty range, which the new value falls into. Sage did have access to high-resolution detectors when he did this experiment in 1976 but he did not use separated isotopes. Pearlstein's value of  $23.3 \pm 2.0$  b can be disregarded because he used natural cadmium and most likely low-resolution detectors, although he does not actually say in his paper.

Heft's thermal cross section value agrees well with the current thermal column result of 2.7 b but not with the rabbit and GRICIT results. However, Heft only used a reactor core source, so he had no thermal neutron source at all. This implies a lack of redundancy in his measurements.

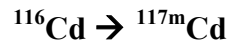


The only previously measured values for  $I$  and  $\sigma$  for this transition were obtained by Seren [16] in 1947. They can be discounted because there were no high-resolution detectors available at that time. It is unclear where Mughabghab obtained his listed value of  $0.036 \pm 0.007$  b. Therefore, the experimentally obtained values of  $\sim 0.05$  b for  $\sigma$  and  $\sim 0.4$  b for the RI can be considered the most accurate cross section values to date.



For this interaction, there are only three previously measured values for the thermal cross section, none of which use high-resolution detectors. The value quoted by Mughabghab of  $0.050 \pm 0.008$  b was obtained by Decat [17] in 1966 using enriched cadmium samples. The values obtained for the RI and  $\sigma$  in present experiment were  $\sim 1.1$  b and  $\sim 0.09$  b. Mughabghab chose to quote a combined calculated value for the  $I$  of the two transitions ( $^{116}\text{Cd} \rightarrow ^{117\text{g}}\text{Cd}$  and  $^{116}\text{Cd} \rightarrow ^{117\text{m}}\text{Cd}$ ) of  $1.5 \pm 0.2$  b so there are no other values to

compare with. However, adding the two I values from the Rabbit together is about 1.4 b, which agrees with Mughabghab's value of 1.5 b.



There are no measured values for the resonance integral for this transition and only one measured value for the thermal cross section obtained after 1960. Mughabghab quotes a calculated value of  $0.025 \pm 0.010$  b for  $\sigma$ , which is similar to Decat's measured value of  $0.027 \pm 0.005$  b. The presently measured value of  $\sim 0.0160$  b falls within the uncertainty of both values.

## V. Conclusions

The neutron capture cross sections of six cadmium isotopes were measured using the neutron activation method, which entails causing neutron capture by the stable isotopes to form radioisotopes. There were two parameters used to describe the cross section as a function of energy. The resonance integral described the cross section of the resonance region, characterized by epithermal neutrons, and the thermal cross section described the end tail of the resonances, characterized by thermal neutrons. For cadmium, the isotope samples needed to be separated to counteract the large cross section of  $^{113}\text{Cd}$  that occurs in the thermal neutron region.

When the presently measured values were compared with previously measured values, it was determined that any disagreement probably stemmed from a difference in the technology available when each measurement was taken or a difference in the method used. A problem for any value obtained before the mid-sixties was a lack of high-resolution detectors, especially for isotopes with complicated decay schemes, such as  $^{117}\text{Cd}$ . Other previous experiments were done through the internal conversion method or by using a ratio of two isotopes for neutron activation. The second of these two methods has more room for error because it relies on a cross section measurement that may or may not be accurate, such as in Beda's  $^{108}\text{Cd}$  thermal cross section measurement. Lastly, the experiments that did not use separated isotope samples can be discounted because of the large effect of  $^{113}\text{Cd}$ .

There were also some discrepancies between the present values obtained for different facilities. Table 4.1 shows a significant difference between the resonance

integral values determined from the CLICIT and from the Rabbit. Without knowing the exact energy dependence of the neutron flux, it is difficult to determine the cause of this difference. Additionally, the TC values for  $^{114}\text{Cd}$  differ by a factor of two from the values determined using the other facilities. The same results were obtained when  $^{114}\text{Cd}$  samples from the Rabbit and GRICIT were re-irradiated in the TC. This indicates that the discrepancy is legitimate and not due to some systematic error, but no possible explanations have been established.

Despite these anomalies, the acquired data are more precise than any data that have been collected before. The high amount of redundancy reached by using different irradiation facilities, the use of high-resolution gamma ray detectors, and the use of separated isotopes are important factors in the accuracy of the values. Attempts to refine the data and explain the discrepancies will continue after the submission of this thesis.

## References

- [1] National Nuclear Data Center: <http://www.nndc.bnl.gov>
- [2] DeSoete, D., Gijbels, R., & Hoste, J. (1972). *Neutron Activation Analysis*. England: John Wiley & Sons, Ltd.
- [3] Krane, K. S. (1988). Nuclear Reactions. *Introductory Nuclear Physics*, 459. New York: John Wiley & Sons, Inc.
- [4] Nuclear Data Sheets: <http://www.nndc.bnl.gov>
- [5] Mughabghab, S.F. (2006). *Atlas of Neutron Resonances*. Amsterdam: Elsevier.
- [6] Anufriev, V., Babich, S., Nefedov, V., & Kocherygin, N. (1984). Parameters of Neutron Resonances of Cadmium-109. *Atomnaya Energiya*, **57**, 59.
- [7] Beda, A., Kondratev, L., & Tret'yakov, E. (1964). The Cross Section of the Activation of Cadmium-108 by Thermal Neutrons. *Soviet Journal of Atomic Energy*, **16**, 145.
- [8] Boyd, H., Hamilton, J., Sattler, A., & Goudsmit, P. (1964). The Thermal Neutron Capture Cross Section of Cadmium-108 and the Decay of Silver-109m. *Physica*, **30**, 124.
- [9] Mangal, S., & Gill, P. (1962). Thermal Neutron Activation Cross-Sections for Isomer Production. *Nuclear Physics* **36**, 542.
- [10] Heft, R. E. (1979). A Consistent Set of Nuclear-Parameter Values for Absolute INAA. *Computers in Activation Analysis and Gamma Ray Spectroscopy; Proceedings of the American Nuclear Society Topical Conference at Mayaguez, Puerto Rico*, 495.
- [11] Van der Linden, R., Hoste, J., & DeCorte, F. (1974). A Compilation of Infinite Dilution Resonance Integrals, II. *Journal of Radioanalytical Chemistry*, **20**, 695.
- [12] Kramer, H. H., & Wahl, W. H. (1965). Formation of Selenium-77m, Selenium-87m, Cadmium-111m and Barium-137m by Reactor Spectrum Neutrons for Use in Activation Analysis. *Nuclear Science and Engineering*, **22**, 373.
- [13] Nakamura, S., Harada, H., & Hayakawa, T. (2009). Measurement of the thermal-neutron capture cross-section and the resonance integral of the  $^{112}\text{Cd}(n,\gamma)^{113\text{m}}\text{Cd}$  reaction. *Japan Atomic Energy Agency Conference: Report JAEA-C-2009-004*.
- [14] Wahl, A. (1959). 14 Year Cd-113m. *Journal of Inorganic and Nuclear Chemistry*, **10**, 1.
- [15] Sage, L., & Furr, K. (1976). The Measurement of Some Resonance Integrals. *Journal of the American Nuclear Society*, **23**, 501.

- [16] Seren, L., Friedlander, H.N., & Turkel, S.H. (1947). Thermal neutron activation cross sections. *Physical Review*, **72**, 888.
- [17] Decat, D., & Del Marmol, P. (1966). Thermal neutron activation cross section of  $^{116}\text{Cd}$  for the production of  $^{117}\text{Cd}$  isomers. *Radiochimica Acta*, **6**, 29.
- [18] Lewis, R. E., & Butler, T. A. (1968). Reactor production and characterization of cadmium-109. *Oakridge National Laboratory Report ORNL-4247*.
- [19] Pearlstein, S., & Milligan, R.F. (1966). Thermal Cross Sections and Resonance Integrals of Cadmium-114. *Journal of Nuclear Science and Engineering*, **26**, 281.
- [20] ORTEC: <http://www.ortec-online.com/Library/index.aspx>

## VI. Appendix

## 6.1 Germanium Single Crystal Diode Detectors

The efficiency parameter in this experiment can be better understood by having an understanding of how the gamma ray detectors work. All germanium detectors use a single crystal of germanium that is grown to have low conductivity, or high resistance. For gamma ray spectroscopy, a coaxial, or cylindrical, geometry is preferred because a large volume of crystal can be used. This type of configuration is seen in Fig. 6.1.

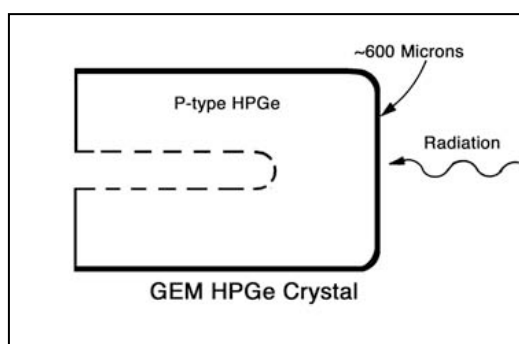


*Figure 6.1: The geometry and components of a p-type GEM HPGe crystal detector. [20]*

A p-type detector has a  $p^+$  contact, which is surrounded by an ion-implanted contact and an  $n^+$  contact. Therefore, a “dead layer” that does not respond to energy is created. Any radiation hitting the detector needs to have enough energy to cause an electron to move from the valence band to the conduction band of the crystal. Then the electron is free to move to the  $n^+$  contact under the influence of an electric field. The number of holes produced in the valence band and the number of electrons added to the conduction band can be measured and used to find the incident energy of the photon. This is possible because the energy required to create an electron-hole pair is known.

When ionizing electromagnetic radiation, such as gamma rays, interacts with a semiconductor detector, three absorption processes can occur: the photoelectric effect, the

Compton effect and pair production. In the photoelectric effect, an incoming photon ejects an electron from the target atom, allowing the electron to move around freely. The Compton effect is an elastic collision between an incoming photon and an electron, in which some of the photon's energy is transferred to the electron. Lastly, pair production occurs when a photon near the nucleus donates its energy to create an electron-positron pair with certain rest mass and kinetic energies.

The efficiency of the detector is defined as the likelihood of incoming radiation interacting with the detector and producing a count. The efficiency value is dependent on the absorption process being detected. In the case of the photoelectric effect, the chance of a gamma ray being detected is greatly influenced by the energy of the incoming photon. Compton scattering is a common occurrence within germanium detectors and the chance of a scattered gamma ray being detected is greatly influenced by the geometry of the detector itself. The subsequent annihilation radiation produced after pair production can escape the detector and cause escape peaks to appear in the spectrum. However, this is only a concern within a high energy range of gamma rays ( $> 1$  MeV) and the highest gamma ray energy considered in the present experiment was  $\sim 1.4$  MeV. All of the absorption processes are dependent on the energy of the gamma ray and the process to determine the efficiency as a function of energy is described in the next section.

## 6.2 Detector Efficiency Curves

The detector efficiency curves were determined in a multi-step process that began with purchasing samples of  $^{152}\text{Eu}$  and  $^{133}\text{Ba}$  with known activities and counting the



gamma rays. These specific elements were chosen because of the energy ranges of gamma rays they emit. Barium emits gamma ray radiation with an energy range of about 100 keV to 500 keV and europium emits gamma ray radiation with an energy range of about 100 keV to 1400 keV. Therefore, the barium was used to calibrate the detector for low energies and europium was used to calibrate the detector for higher energies.

The peak areas for each element were determined by Maestro, and the activity was found using the same Excel template method as for determining the cross section. The activity, peak area, run time and branching ratio for each individual gamma ray were all plugged into Eq. 3.1. A plot of efficiency as a function of energy could be made for the high and low energy ranges, however the plots are easier to interpret on a log scale. When the natural log is taken of both sides, the low energy plot turns into a 4<sup>th</sup> or 5<sup>th</sup> degree polynomial function and the high energy plot turns into a simple linear relationship with a negative slope. Fig. 6.2 is the low energy plot and Fig. 6.3 is the high energy plot. These log-functions were used to determine the efficiency for the gamma ray energies of the relevant cadmium isotopes.

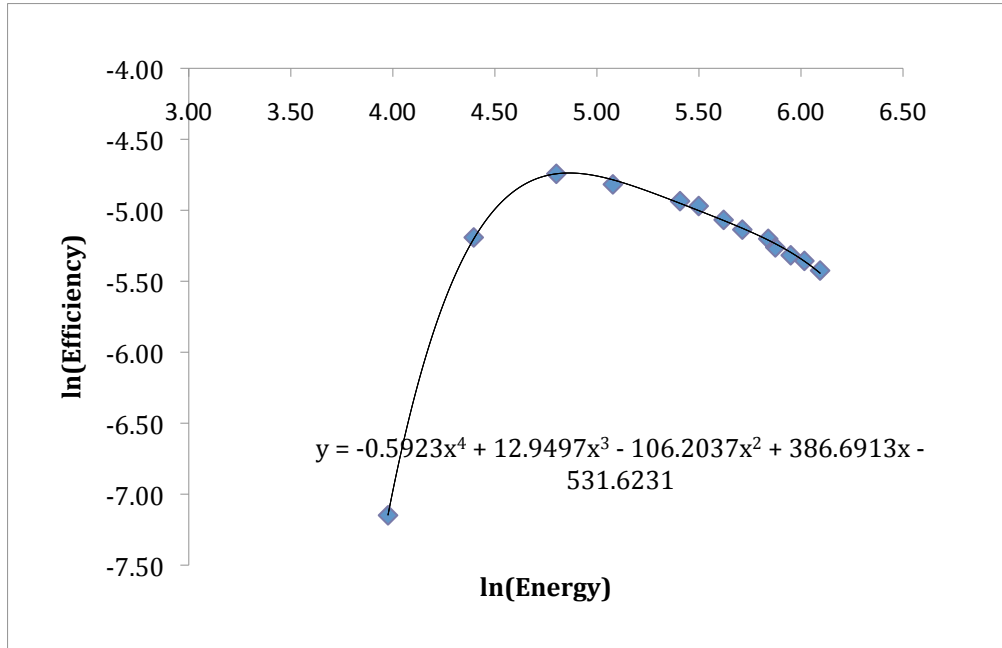


Figure 6.2: The low energy (0-500 keV) efficiency curve for detector 1 (D1) at 10 cm. The equation for the trend line is shown.

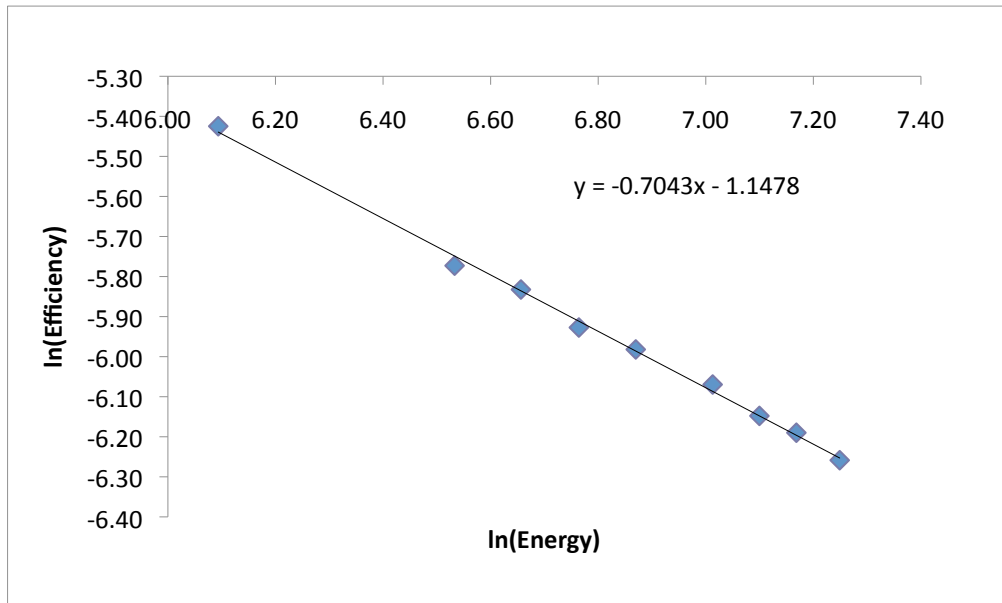


Figure 6.3: The high energy (>500 keV) efficiency curve for D1. The equation for the trend line is shown.

The efficiencies for gamma rays of energies at about 100-200 keV were harder to determine with as much precision as higher or lower energies because of the shape of the low energy efficiency plot. Between 90 and 250 keV on the  $\ln(\text{Energy})$  axis there is a

curve of the data that could be fitted with several different degrees of polynomials. Therefore, the efficiencies in this area are subject to the greatest margin of error. The efficiencies for the higher energy gammas had the least margin of error due to the linear relationship between energy and efficiency.

### 6.3 Neutron Fluxes

For every facility used for irradiation, the exact thermal and epithermal neutron fluxes needed to be known. The process for calculating the neutron flux is the same as the process for calculating the cross section, except the fluxes are the unknowns and the resonance integral and thermal cross section can be found in literature. Gold, cobalt and zirconium samples, with known neutron capture cross sections, were irradiated alongside the cadmium samples in every facility. The activities were determined and Eq. 2.6 was solved for the thermal or epithermal flux. The final results are compiled in Table 6.1.

*Table 6.1: Values for the thermal and epithermal fluxes of each irradiation facility in the OSU TRIGA reactor. It is important to note that the CLICIT, Rabbit 2 and Rabbit 4 have thermal fluxes of zero and that all the flux values for the Rabbit are the same.*

	<b>Thermal Flux (n/cm<sup>2</sup>/s)</b>	<b>Epithermal Flux(n/cm<sup>2</sup>/s)</b>
<b>CLICIT</b>	0	1.13x10 <sup>12</sup>
<b>GRICIT</b>	4.4x10 <sup>12</sup>	3.5x10 <sup>11</sup>
<b>Thermal Column</b>	8.7x10 <sup>10</sup>	2.0x10 <sup>8</sup>
<b>Rabbit 1</b>	7.8x10 <sup>12</sup>	3.5x10 <sup>11</sup>
<b>Rabbit 2 (Cd)</b>	0	3.5x10 <sup>11</sup>
<b>Rabbit 3</b>	7.8x10 <sup>12</sup>	3.5x10 <sup>11</sup>
<b>Rabbit 4 (Cd)</b>	0	3.5x10 <sup>11</sup>

## 6.4 Error Analysis

There were many factors that contributed to the overall error values of the present results. The abundance of the isotope within the sample, the mass of the sample, the half-life of the state experiencing decay, the branching ratio of each gamma ray, the statistics of the Maestro program, the efficiency of the detector and the accuracy of the neutron flux all had to be taken into account. The exact percent error values were estimated if they could not be found in the literature.

The values for the abundance, the half-life and the branching ratio were all easily determined from some other source. Error in the sample abundance was given by the manufacturer of the cadmium samples, and the half-life and branching ratios errors were looked up in the Nuclear Data Sheets [1]. The statistics of Maestro's peak area value were determined automatically by the Excel template using the chi-square method of error analysis. The mass values were determined based on the size of the sample and the smallest increment of measurement on the scale, which happened to be ~0.1 mg. Calculating the error values for the flux and efficiency was more complicated because they both are affected by the error values for all the other parameters. Therefore, these values could be found by determining a deviation from the average value when other parameters were changed. Table 6.2 is a compilation of all the exact error values for each state of each isotope.

The percent error totals were found by taking the square root of the sum of the squares of each parameter. Calculating the error for the GRICIT samples and the Rabbit samples without any Cd container were slightly more complicated due to the fact that their cross section values relied on an experimental resonance integral value. The

uncertainty in the thermal cross section values found using these facilities had to take into account the uncertainty of the resonance integral as well. This was accomplished by simply determining the change in  $\sigma$  as the  $I$  value was changed.

*Table 6.2: A compilation of the percent error associated with each isotope due to a variety of factors.*

<b>CLICIT</b>	<b>107</b>	<b>109</b>	<b>111m</b>	<b>113</b>	<b>115g</b>	<b>115m</b>	<b>117g</b>	<b>117m</b>
Abundance	1	0.1	0.1	0.1	0.1	0.1	0.23	0.23
mass	1.2	1.2	1.2	0.25	0.5	0.5	1.2	1.2
half-life	0.33	0.25	0.19	3.5	0.5	0.1	0.3	0.4
statistics	1	0.3	0.1	6	0.01	0.5	0.5	0.5
branch	5	3	3	3	2	35	1	1
efficiency	0.5	1	1	1	0.5	0.5	0.5	0.5
flux	3	3	3	3	3	3	3	3
total	6.15	4.54	4.53	8.21	3.71	35.14	3.48	3.49
<b>Rabbit-Cd</b>								
Abundance	1	0.1	0.1		0.1	0.1	0.23	0.23
mass	1.2	1.2	1.2		0.5	0.5	1.2	1.2
half-life	0.33	0.25	0.19		0.5	0.1	0.3	0.4
statistics	5	1.5	0.2		0.1	5	0.1	0.3
branch	5	3	3		2	35	1	1
efficiency	0.5	1	1		0.5	0.5	0.5	0.5
flux	3	3	3		3	3	3	3
total	7.86	4.77	4.53		3.71	35.49	3.44	3.46
<b>TC</b>								
Abundance	1	0.1	0.1		0.1	0.1	0.23	0.23
mass	1.2	1.2	1.2		0.5	0.5	1.2	1.2
half-life	0.33	0.25	0.19		0.5	0.1	0.3	0.4
statistics	6	3	0.4		0.1	2	0.7	0.25
branch	5	3	3		2	35	1	1
efficiency	0.5	1	1		0.5	0.5	0.5	0.5
flux	3	3	3		3	3	3	3
total	8.53	5.43	4.54		3.71	35.19	3.51	3.46
<b>GRICIT</b>								
Abundance	1	0.1	0.1	0.1	0.1	0.1	0.23	0.23
mass	1.2	1.2	1.2	0.25	0.5	0.5	1.2	1.2
half-life	0.33	0.25	0.19	3.5	0.5	0.1	0.3	0.4
statistics	2	0.6	0.2	7	0.02	0.3	0.1	0.3
branch	5	3	3	3	2	35	1	1
efficiency	0.5	1	1	1	0.5	0.5	0.5	0.5
flux	3	3	3	3	3	3	3	3
RI unc	1.6	3.3	1.72		1.1	11.3	1.6	3
total	6.58	5.64	4.85	8.96	3.87	36.91	3.80	4.58
<b>Rabbit</b>								
Abundance	1	0.1	0.1		0.1	0.1	0.23	0.23
mass	1.2	1.2	1.2		0.5	0.5	1.2	1.2
half-life	0.33	0.25	0.19		0.5	0.1	0.3	0.4
statistics	2	1	0.1		0.02	1	0.1	0.4
branch	5	3	3		2	35	1	1
efficiency	0.5	1	1		0.5	0.5	0.5	0.5
flux	3	3	3		3	3	3	3
RI unc	1	1	0.8		0.4	4.3	0.5	0.8
total	6.47	4.74	4.60		3.73	35.41	3.48	3.56

## **VII. Acknowledgments**

There are several people I would like to acknowledge for helping me through this challenging experience. Firstly, I want to thank my advisor Dr. Krane for being patient and available through the whole process and giving me such an awesome opportunity. I would like to thank Dr. Tate for being so invested in the success of her students and for always reminding us to get an early start. And lastly, I would like to say thanks to my mom and dad for providing me with unconditional love and support no matter what.